

## Research



**Cite this article:** Gondwe MJ, Helfter C, Murray-Hudson M, Levy PE, Mosimanyana E, Makati A, Mfundisi KB, Skiba UM. 2021 Methane flux measurements along a floodplain soil moisture gradient in the Okavango Delta, Botswana. *Phil. Trans. R. Soc. A* **379**: 20200448. <https://doi.org/10.1098/rsta.2020.0448>

Accepted: 9 July 2021

One contribution of 12 to a discussion meeting issue 'Rising methane: is warming feeding warming? (part 1)'.

**Subject Areas:**

biogeochemistry, environmental chemistry, atmospheric science, ecosystems

**Keywords:**

seasonal floodplains, methane emissions, methane oxidation, occasional floodplains, tropical wetland

**Author for correspondence:**

M. J. Gondwe

e-mail: [mgondwe@ub.ac.bw](mailto:mgondwe@ub.ac.bw)

Electronic supplementary material is available online at <https://doi.org/10.6084/m9.figshare.c.5568328>.

Methane flux measurements  
along a floodplain soil  
moisture gradient in the  
Okavango Delta, Botswana

M. J. Gondwe<sup>1</sup>, C. Helfter<sup>2</sup>, M. Murray-Hudson<sup>1</sup>,  
P. E. Levy<sup>2</sup>, E. Mosimanyana<sup>1</sup>, A. Makati<sup>1</sup>,  
K. B. Mfundisi<sup>1</sup> and U. M. Skiba<sup>2</sup>

<sup>1</sup>Okavango Research Institute, University of Botswana, P/Bag 285, Maun, Botswana

<sup>2</sup>UK Centre for Ecology and Hydrology, Atmospheric Chemistry and Effects, Bush Estate, Penicuik EH26 0QB, UK

MJG, 0000-0002-2607-5399; CH, 0000-0001-5773-4652

Data-poor tropical wetlands constitute an important source of atmospheric CH<sub>4</sub> in the world. We studied CH<sub>4</sub> fluxes using closed chambers along a soil moisture gradient in a tropical seasonal swamp in the Okavango Delta, Botswana, the sixth largest tropical wetland in the world. The objective of the study was to assess net CH<sub>4</sub> fluxes and controlling environmental factors in the Delta's seasonal floodplains. Net CH<sub>4</sub> emissions from seasonal floodplains in the wetland were estimated at  $0.072 \pm 0.016 \text{ Tg a}^{-1}$ . Microbial CH<sub>4</sub> oxidation of approximately  $2.817 \times 10^{-3} \pm 0.307 \times 10^{-3} \text{ Tg a}^{-1}$  in adjacent dry soils of the occasional floodplains accounted for the sink of 4% of the total soil CH<sub>4</sub> emissions from seasonal floodplains. The observed microbial CH<sub>4</sub> sink in the Delta's dry soils is, therefore, comparable to the global average sink of 4–6%. Soil water content (SWC) and soil organic matter were the main environmental factors controlling CH<sub>4</sub> fluxes in both the seasonal and occasional floodplains. The optimum SWC for soil CH<sub>4</sub> emissions and oxidation in the Delta were estimated at 50% and 15%, respectively. Electrical conductivity and pH were poorly correlated ( $r^2 \leq 0.11$ ,  $p < 0.05$ ) with CH<sub>4</sub> fluxes in the seasonal floodplain at Nxaraga.

This article is part of a discussion meeting issue 'Rising methane: is warming feeding warming? (part 1)'.

## 1. Introduction

Global warming is associated with increasing atmospheric concentrations of greenhouse gases (GHGs) such as nitrous oxide (N<sub>2</sub>O), carbon dioxide (CO<sub>2</sub>) and methane (CH<sub>4</sub>) [1–3]. Methane is currently the second most abundant GHG in the atmosphere after CO<sub>2</sub> [4]. In the period between 1800 and the 1990s atmospheric concentrations of CH<sub>4</sub> increased; then stabilized at approximately 1775 ppb between 1999 and 2006 [5,6]. Renewed growth in global atmospheric CH<sub>4</sub> concentrations started in 2007 [6–8]. The reasons for the stabilization and the renewed growth of approximately 6 Tg CH<sub>4</sub> a<sup>-1</sup> or approximately 3% increase in atmospheric CH<sub>4</sub> concentration per year [9,10] since 2007 remain poorly understood due to seemingly contradictory findings, especially pertaining to the magnitudes of CH<sub>4</sub> sources estimated using different methods, by various research works on the issue [6,9,10].

According to Dlugokencky and colleagues [8,10], the 2007 renewed growth in atmospheric CH<sub>4</sub> concentration is consistent with abrupt increases in CH<sub>4</sub> emissions from biomass burning and wetlands as well as a reduction in the tropospheric hydroxyl radical (OH) sink of CH<sub>4</sub>. Tropical and subtropical wetlands remain the world's largest natural source of CH<sub>4</sub> to the atmosphere [11,12], accounting for 70% of the global wetland emissions budget [12,13]. However, estimates of natural CH<sub>4</sub> sources and sinks, particularly in the South American, African and Asian tropics, remain poorly constrained, and with uncertain attribution to the various biogenic and anthropogenic sources [14,15], thereby hindering development and evaluation of regional and global CH<sub>4</sub> budgets. Methanotrophic CH<sub>4</sub> oxidation, the only known biological sink of atmospheric CH<sub>4</sub>, is also poorly understood [16] despite accounting for 4–6% of the total atmospheric CH<sub>4</sub> sink [17].

The aim of this study was to address the uncertainty of CH<sub>4</sub> fluxes, particularly net CH<sub>4</sub> fluxes and controlling environmental factors, from the alluvial Okavango Delta wetlands in Botswana, which is the world's sixth largest wetland. The Okavango Delta consists of permanent and seasonal wetlands bordering onto dry, occasionally flooded grassland and forest areas (figure 1*a*). We report the first chamber-based CH<sub>4</sub> flux measurements along a soil moisture gradient in a seasonal floodplain in the Okavango Delta.

## 2. Material and methods

### (a) Study site

The Okavango Delta (figure 1*a*) is an alluvial wetland with a total area of approximately 22 000 km<sup>2</sup> and a very low average gradient (1:3600) [18]. The Delta is recharged by flood-pulsed inflow of approximately 10 × 10<sup>9</sup> m<sup>3</sup> a<sup>-1</sup> (range of 7–15 × 10<sup>9</sup> m<sup>3</sup> a<sup>-1</sup>; [19,20]) via the Okavango River which drains the central Angolan highlands located in a subtropical and humid climate with precipitation of up to 1300 mm a<sup>-1</sup> [21,22]. An additional water input into the Delta comes from seasonal, erratic and localized convective rainfall over the wetland area averaging 490 mm a<sup>-1</sup> (equivalent to 6 × 10<sup>9</sup> m<sup>3</sup> a<sup>-1</sup>) between December and April, peaking in February [20]. Due to the semi-arid conditions in the region, annual evapotranspiration in the Delta exceeds precipitation by a factor of more than 3, such that the system loses 98% of the total water inflow to the atmosphere. The remaining 2% exits the Delta as river outflow through the Boro/Thamalakane and Kunyere Rivers (figure 1) [19,23].

The Delta can be divided into three broad ecological zones based on their hydroperiods: the permanent swamp, the seasonal floodplains and the occasional floodplains (figure 1*a*). The permanent swamp, which covers a maximum area of about 3000 km<sup>2</sup>, consists of the Panhandle

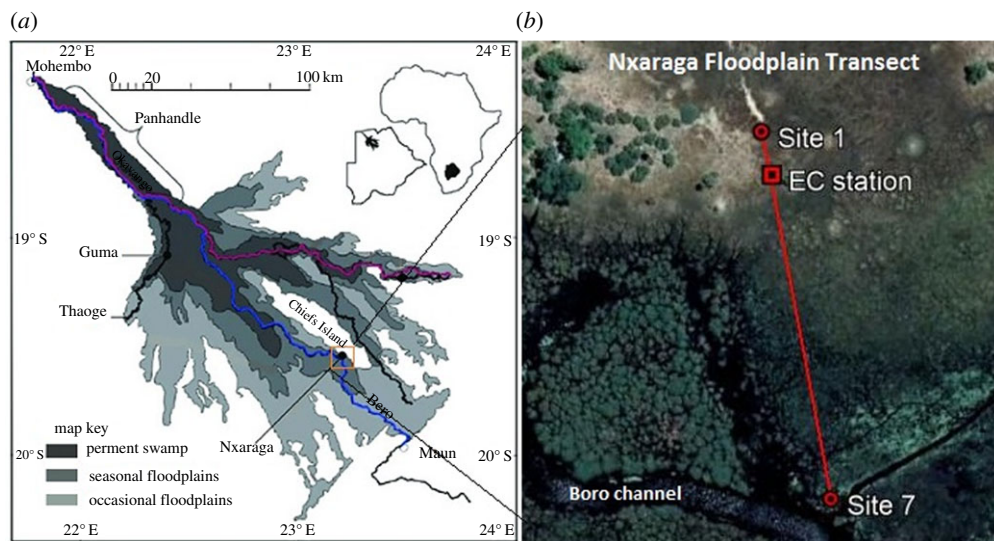


**Figure 1.** Map of the Okavango Delta (a) showing the study location and study transect across the seasonal floodplain at Nxaraga (b). The transect was oriented along the predominant southerly wind direction at Nxaraga. (Online version in colour.)

and the upper fan area, and is sustained by a base flow of approximately  $150 \text{ m}^3 \text{ s}^{-1}$  of the Okavango River [21]. The permanent swamp is dominated by dense vegetation stands composed of mainly *Cyperus papyrus* and *Phragmites australis* [20]. Most of the flood water in the swamp flows laterally through the dense vegetation [20], which, together with the low gradient, significantly decrease water velocity through the swamp, and consequently sediment and nutrient transport into the seasonal floodplains [24].

The flooding of the southern distal areas of the alluvial fan creates seasonal floodplains, which typically last for six to eight months depending on local summer rainfall and annual volume of inflow via the Okavango River. The seasonal floodplains can cover a total area of more than  $3000 \text{ km}^2$  [25], but flooding extents in excess of  $6000 \text{ km}^2$  have also been reported (see [26]). The flooding is followed by a burst of plant growth dominated by reeds (*Phragmites* spp.) and aquatic herbs (e.g. *Nymphaea* spp., *Potamogeton thunbergii*) in areas subject to longer and deeper floods (e.g. channels and lagoons), and sedges (e.g. *Cyperus articulatus*, *Schoenoplectus corymbosus*) in regularly inundated floodplain areas while grasses (e.g. *Miscanthus junceus*, *Panicum repens*, *Oryza longistaminata* and *Leersia hexandra*) dominate at the floodplain-woodland fringes [27–29]. Dry floodplain fringes are typically dominated by broad-leaved evergreen trees such as *Croton megalobotrys*, *Diospyros mespiliformis*, *Garcinia livingstonei* and *Ficus sycomorus* [30], while occasionally flooded areas (approx. once in a decade) in more distal locations are usually dominated by grasses such as *Urochloa* sp., *Eragrostis* spp. and *Aristida* spp. [27]. The plant species composition is, therefore, dependent on zone topography and hydroperiod across the floodplain areas [30,31]. The seasonal floodplains are heavily used for grazing and water by large numbers of wildlife species especially during the dry season when forage and water are scarce in the surrounding upland areas [32].

A substantial amount of water is lost to the atmosphere through evapotranspiration in the seasonal floodplains especially during maximum inundation. The evapotranspirative water loss by plants results in the accumulation of solutes (e.g. calcium, magnesium, potassium, silica and sodium) and nutrients (e.g. nitrogen and phosphorus) in soil water particularly under islands fringed by a variety of broad-leaved, evergreen trees and shrubs (see above). The evapotranspirative removal of solutes and nutrients from floodplain surface waters maintains the Okavango Delta as a freshwater system despite centuries of solute loading [33,34]. Most seasonal

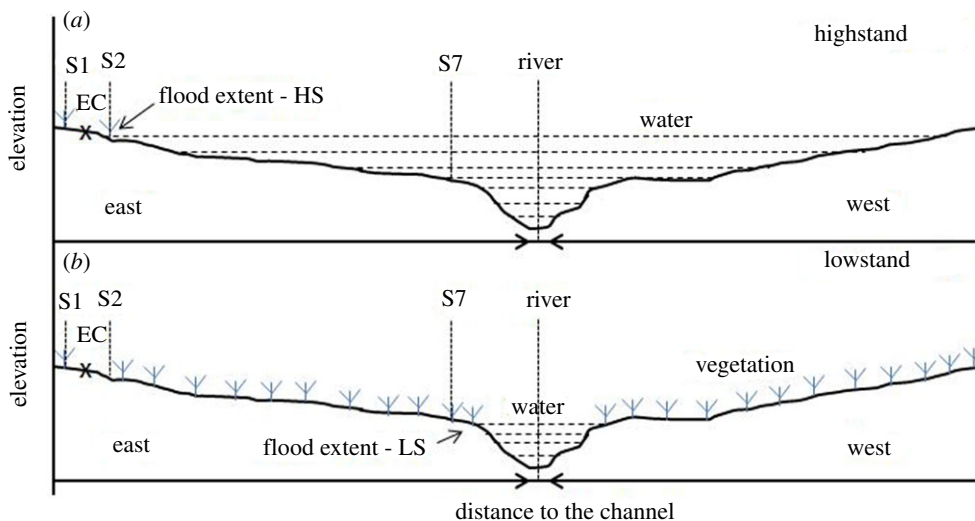


**Figure 2.** Schematic diagram of the highstand (a) and lowstand (b) flood extents in the seasonal floodplain at Nxaraga. The flood extent during a particular sampling campaign determined the length of that campaign's sample transect across the seasonal floodplain. The sample transect was longest at lowstand and shortest at highstand flood extents. For plant species and distribution across a seasonal floodplain see [27]. (Online version in colour.)

floodplains in the Okavango Delta experience regular fire activities during the dry winter period between May and September, which consumes most of the above ground dry vegetation and litter [35].

The high level of herbivory, low incident rainfall, infertile sandy soils and frequent fire events result in low accumulation of vegetation biomass in these seasonal floodplains compared to the permanent swamps [35]. In addition, the organic matter accumulated during wet periods may experience extensive aerobic decomposition during the dry season [36]. The arenosols consist predominantly of sands (up to 85% [37]) with an increase in peat and other organic material as distance to the river channel decreases thus creating an 'O' horizon in the lower seasonal floodplains. The predominant soils in this region are bright, well-drained sands or loamy sands (Haplic Arenosols) and dark greyish brown, poorly drained sandy loams or clays (Eutric Gleysols) [38].

We established a spatial transect to study soil CH<sub>4</sub> emissions using closed chambers in a seasonal floodplain at Nxaraga (figure 1b) on the southwest side of the Chief's Island in the Okavango Delta, Botswana. The floodplain is bounded to the west by the Boro River, which is one of the main channel systems and outlets of the Delta. The transect was constructed to span dry to waterlogged soils across the floodplain following the moving flood water edge (figure 2). Site 1 (19°32'52.40" S, 23°10'44.75" E) on rarely flooded dry soils was the only fixed site on the transect because it remained accessible throughout the sampling period (figure 1b). Site 2 slightly fluctuated but was basically located at the edge of the floodplain (where the water front reached) at highstand. Locations of Sites 3–7 depended on the length of the remainder of the transect which was equally portioned into additional two to five sites, partly determined by visual changes (especially wetness) in substrate conditions. The number of measurement sites, therefore, varied from a maximum of seven sampling sites at lowstand (during the peak of the dry season) to a minimum of four sampling sites at highstand (at maximum flooding extent) (figure 2). A total of 16 field campaigns were conducted over a 2-day period almost monthly from February 2018 to August 2020. Sampling was, however, not done regularly according to plan (monthly) due to unforeseen circumstances, primarily poor accessibility (by boat and vehicle) of the seasonal floodplain from Maun during certain seasons.

## (b) Measurements of CH<sub>4</sub> fluxes

CH<sub>4</sub> fluxes were measured using a closed dynamic chamber system comprising a transparent cylindrical polycarbonate chamber (388 mm dia., 305 mm high) placed on a pre-installed base, coupled to an ultra-portable GHG Analyzer (GGA, model 915-0011, Los Gatos Research (LGR), Mountain View, CA, USA). The performance of the generally robust GGA was checked at the UK-CEH for compliance with the World Meteorological Organization (WMO) requirements prior to the field campaign in the Okavango Delta, Botswana, using 3-point concentration standards calibrated relative to the WMO CH<sub>4</sub>-X2004 scale and WMO CO<sub>2</sub>-X2007 scale for CH<sub>4</sub> and CO<sub>2</sub>, respectively. In the field, a set of three plastic chamber bases were installed at each site along the transect at least 12 h prior to gas measurements; these were removed soon after the measurements to avoid trampling by wildlife. The flow rate through the GGA absorption cell during measurements was 0.5 l min<sup>-1</sup> and the chamber + tubing volume to surface area ratio was 30.5 cm<sup>3</sup> cm<sup>-2</sup>. The air in the chamber was continuously mixed during measurements using a compact fan mounted on the lid of the chamber. The chamber operated as a closed system, meaning that the sample air was continuously withdrawn from the chamber headspace, passed through the GGA for simultaneous CO<sub>2</sub>, CH<sub>4</sub> and H<sub>2</sub>O measurements and returned to the chamber. Each chamber measurement lasted 10 min and the GGA reported gas concentrations as dry mole fractions in ppm at 8 s intervals. The use of the GGA offers several advantages over laboratory gas chromatographs (GCs) commonly used to measure GHG fluxes. For instance, the sensitivity of infrared spectrometer technology used in the GGA is 500 times better than that of most GCs [39], accurate measurements of multiple gaseous components are taken in real time, the number of measurements obtained for calculating fluxes is many times larger, and a shorter enclosure time can be used. Diurnal variations were very small [40].

CH<sub>4</sub> fluxes from the seasonal floodplain were also measured using eddy-covariance equipment deployed along the study transect (figure 1b) as a separate but complementary project reported elsewhere [41], except for comparison with the chamber-based fluxes.

## (c) Flux calculation

For each chamber measurement, the flux of CH<sub>4</sub> was estimated from the time series of CH<sub>4</sub> mixing ratio (nmol mol<sup>-1</sup>) with time. Because the response often deviates from linear, the initial rate of change  $dC/dt$  at  $t=0$  has to be inferred from the data using an appropriate model. Here, we fitted four models to the data (linear, quadratic, asymptotic and the HMR models [42]) and used the approach of Levy *et al.* [43] to choose the most appropriate estimate, based on goodness-of-fit criteria. Fluxes were calculated using the R statistical software (R Foundation for Statistical Computing, Vienna, Austria). For plotting and statistical analysis, Sigmaplot 14.0 software (Systat Software Inc., San Jose, CA, USA) was used.

## (d) Soil measurements

Soil temperature was measured next to the chamber base at a depth of approximately 10 cm using a Hygipal digital thermometer (model GH628 with accuracy of  $\pm 1^\circ\text{C}$ ) during each chamber measurement event. After flux measurements were completed, soil samples (0–10 cm depths) were cored inside each chamber base, using a regular soil auger, and stored in airtight double-zipper plastic bags, yielding three sediment/soil cores at each site. These samples were analysed for soil pH, electrical conductivity (EC), soil water content (SWC) and soil organic matter (SOM) content using standard methods at the Environmental Laboratory, Okavango Research Institute, Maun, Botswana. Soil pH was determined potentiometrically according to Hendershot *et al.* [44] using a pH meter (WTW Inolab pH7110, Weilheim, Germany) after suspension in 1:2.5 (m/v) soil/water ratio. Soil EC was measured 2 h later on the same 1:2.5 (m/v) soil/water suspension using a WTW Inolab Cond7110 metre, Weilheim, Germany [45]. SWC and SOM were determined using gravimetric methods and reported on a dry weight basis. SWC, defined as the ratio of the

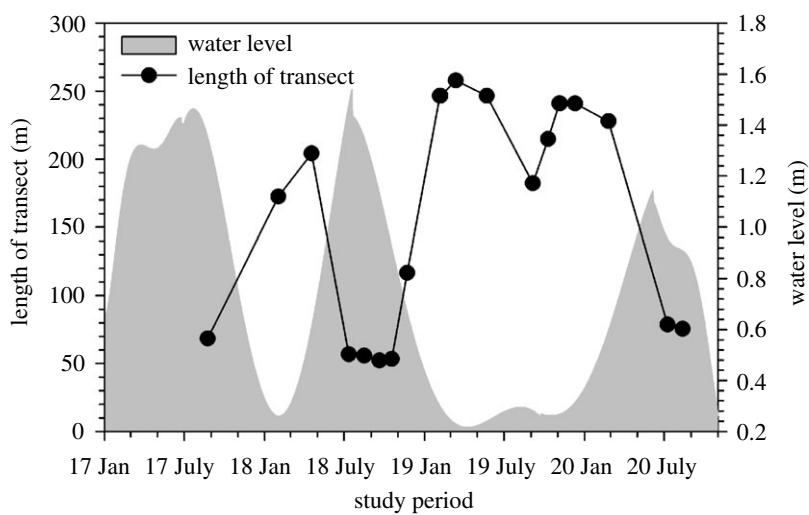


**Figure 3.** Variations in the length of the sampling transect due to seasonal flooding illustrated by water level in the bordering Boro channel at Nxaraga (figure 1*b*). Transects spanned Site 1 (at 0 m transect length) to the flood water front or edge of Boro channel (dark circles) as the water expanded or receded in the floodplain. Longest (e.g. greater than 200 m) and shortest (approx. 50 m) transects were, respectively, sampled during lowstand and highstand flood extents in the seasonal floodplain. See figure 2 for a schematic diagram of the floodplain cross-section at highstand and lowstand flood extents.

mass of water present to the dry weight of the soil sample, was determined using homogeneously mixed wet soil subsamples weighed before and after drying to constant weight at 105°C for 24 h in a Scientific Series 2000 oven (RSA). SOM was estimated by weight loss-on-ignition [46]. A previously oven-dried (at 105°C) soil subsample ( $5.000 \pm 0.005$  g) was combusted in a Carbolite muffle furnace (UK) at 550°C for 2 h in pre-weighed clean ceramic porcelain crucibles, cooled to room temperature and reweighed. SOM (%) was calculated as the difference between the oven-dry soil mass and the soil mass after combustion at 550°C, divided by the oven-dry soil mass.

### 3. Results

The length of the transect which was not inundated (figure 1*b*) ranged from approximately 52 m at maximum flooding (highstand) to 260 m at minimum flooding (lowstand) (figure 3). Soil temperature across the floodplain transect during the study period was recorded at  $24.8 \pm 0.8^\circ\text{C}$  (mean  $\pm$  s.e.).

Site 1 was characterized by dry soils, and patches of salt deposits, common in central areas of most islands in the Okavango Delta, were conspicuous at the soil surface. Because of this, a much higher soil EC value (mean  $\pm$  s.e.) of  $578.3 \pm 75.7 \mu\text{S cm}^{-1}$  was recorded at Site 1 compared to a mean of  $91.6 \pm 8.3 \mu\text{S cm}^{-1}$  observed at the other measurement sites along the floodplain transect. During 12 of the 16 monthly sampling campaigns, we observed a gradient of decreasing EC values along the transect from Site 1 to the flood water front (figure 4*a*). Soil pH showed an exponential decline from dry soils at Site 1 to the river channel (figure 4*b*). Soil pH was significantly higher ( $p < 0.05$ ) at Site 1 ( $9.6 \pm 0.1$ ) than the mean pH of  $5.7 \pm 0.1$  at the other sites along the floodplain transect.

SWC and SOM increased with distance along the floodplain transect to the river channel (figure 5*a,b*). The mean SWC and SOM recorded at Sites 1 and 2 were  $13.40 \pm 1.13\%$  SWC and  $4.90 \pm 0.71\%$  SOM, which increased to  $73.28 \pm 7.01\%$  SWC and  $16.12 \pm 1.42\%$  SOM between Sites 5 and 7. SWC and SOM values at littoral floodplain sites (Sites 1, 2 and 3 at 0, 40 and 70 m average distance along the transect, respectively) tended to be negatively correlated ( $r^2 = 0.4646$ ,  $p < 0.05$

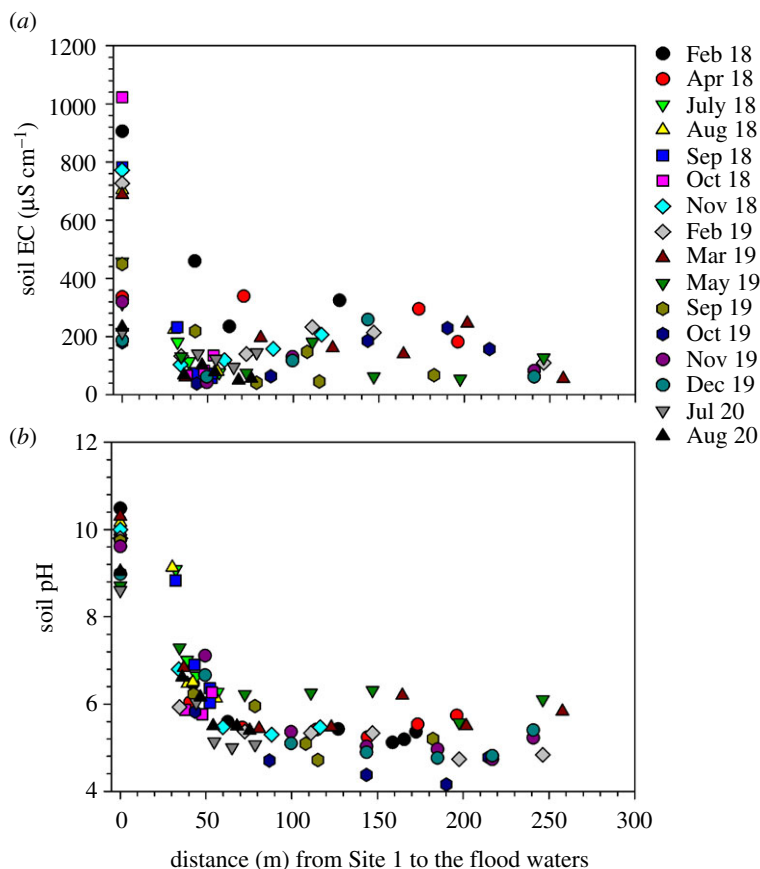


**Figure 4.** Variations of soil EC (a) and soil pH (b) along a transect (Sites 1–7) across a seasonal floodplain at Nxaraga. The data are the means of three replicates per sampling site for soil pH and soil EC obtained during the monthly 2-day sampling campaigns. The legend will be the same for the rest of the figures unless legend is provided for that figure. (Online version in colour.)

at Site 3; figure 6a), but positively correlated ( $r^2 = 0.4694$ ,  $p < 0.05$ ) at the lower floodplain Sites 4–7 (figure 6b). In general, aggregated SWC and SOM data from Sites 1–7 were positively correlated ( $r^2 = 0.5469$ ,  $p < 0.05$ ; figure 6c).

Methane emissions increased from the littoral site (Site 1) to the flood water front during all sampling campaigns (figure 7a). The mean  $\text{CH}_4$  flux rate for all samples collected at Sites 2–7 during the whole sampling campaign between February 2018 and August 2020 was  $44.89 \pm 10.80 \text{ nmol m}^{-2} \text{ s}^{-1}$ . By contrast,  $\text{CH}_4$  oxidation was primarily recorded at Site 1 (and sporadically at Site 2), and the mean flux was  $-0.79 \pm 0.09 \text{ nmol m}^{-2} \text{ s}^{-1}$ .

Soil pH and EC were poorly correlated ( $r^2 \leq 0.11$ ) with  $\text{CH}_4$  fluxes (figure 7b,c). However, emissions were generally higher (greater than  $100 \text{ nmol CH}_4 \text{ m}^{-2} \text{ s}^{-1}$ ) between pH 5.0 and pH 6.6 and EC of less than  $200 \mu\text{S cm}^{-1}$ .  $\text{CH}_4$  emissions showed a tendency to increase as SOM (figure 8a) and SWC (figure 9a) increased along the study transect. Similarly  $\text{CH}_4$  oxidation increased, especially at Site 1, as SOM and SWC increased from 2% to 5% (figure 8b) and 3% to 15% (figure 9b), respectively. Higher SOM and SWC favoured  $\text{CH}_4$  emission rather than oxidation.

Soil  $\text{CH}_4$  fluxes measured by the closed chamber technique agreed reasonably well with their eddy-covariance counterparts in 2018 and 2019 (figure 10). To facilitate the comparison between the two techniques, eddy-covariance data were selected for monthly averaging if the flux footprint was consistent with the portion of the floodplain where chamber measurements took place. Without that condition on the extent of the flux footprint, the eddy-covariance fluxes were an order of magnitude larger than the chambers values in 2019, but still comparable in 2018.

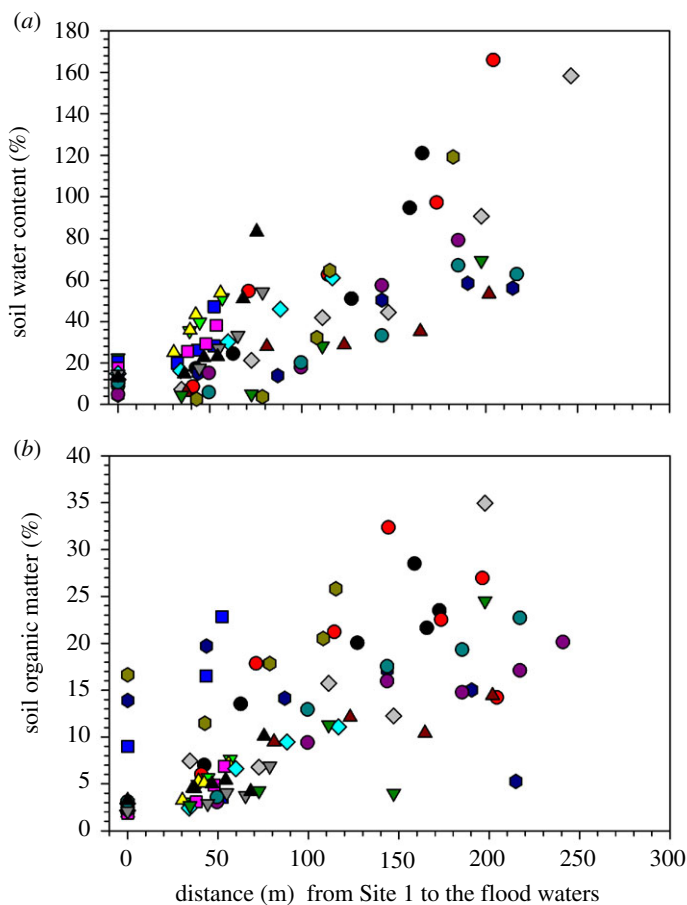


**Figure 5.** Variations of soil water content (*a*) and soil organic matter (*b*) along a transect (Sites 1–7) across a seasonal floodplain at Nxaraga. The data are the means of three replicates per sampling site for SWC and SOM obtained during the monthly 2-day sampling campaigns. See figure 2 for legend. (Online version in colour.)

## 4. Discussion

The data reported here spans the period from February 2018 to August 2020. During this period, the Okavango Delta experienced a significant reduction in annual water inflow via the Okavango River. For instance, the maximum inundation extent in the Delta estimated from MODIS imagery [47] declined from greater than 11 000 km<sup>2</sup> in 2010–2012 to less than 3500 km<sup>2</sup> in 2019 ([http://www.okavangodata.ub.bw/ori/monitoring/flood\\_maps/](http://www.okavangodata.ub.bw/ori/monitoring/flood_maps/)). Consequently most seasonal floodplains, including Nxaraga floodplain, received little or no flooding especially during the 2019 flood season. The drought is likely to have affected biogeochemical processes in the floodplain soils including decomposition of organic matter, CH<sub>4</sub> production and oxidation, and net fluxes [48,49].

The influence of pH on methanogenic and methanotrophic microbial activities is dynamic. For example, Valentine *et al.* [50] found a correlation between pH and potential CH<sub>4</sub> production in laboratory experiments, while Moore & Knowles [51] found no relationship. At the global scale, Wen *et al.* [52] reported that temperature and soil pH are major controllers of methanogenesis. At Nxaraga seasonal floodplain, pH across the transect varied widely and ranged from pH 4.2 to 10.5. The pH decreased from dry soils at Site 1 to the edge of the Boro channel, as previously reported by Bonyongo *et al.* [53]. The variability was much larger across the lower floodplain area (pH 4.2–9.1 between Sites 2 and 7) than at the dry soil Site 1 (pH 8.6–10.5). According to Segers



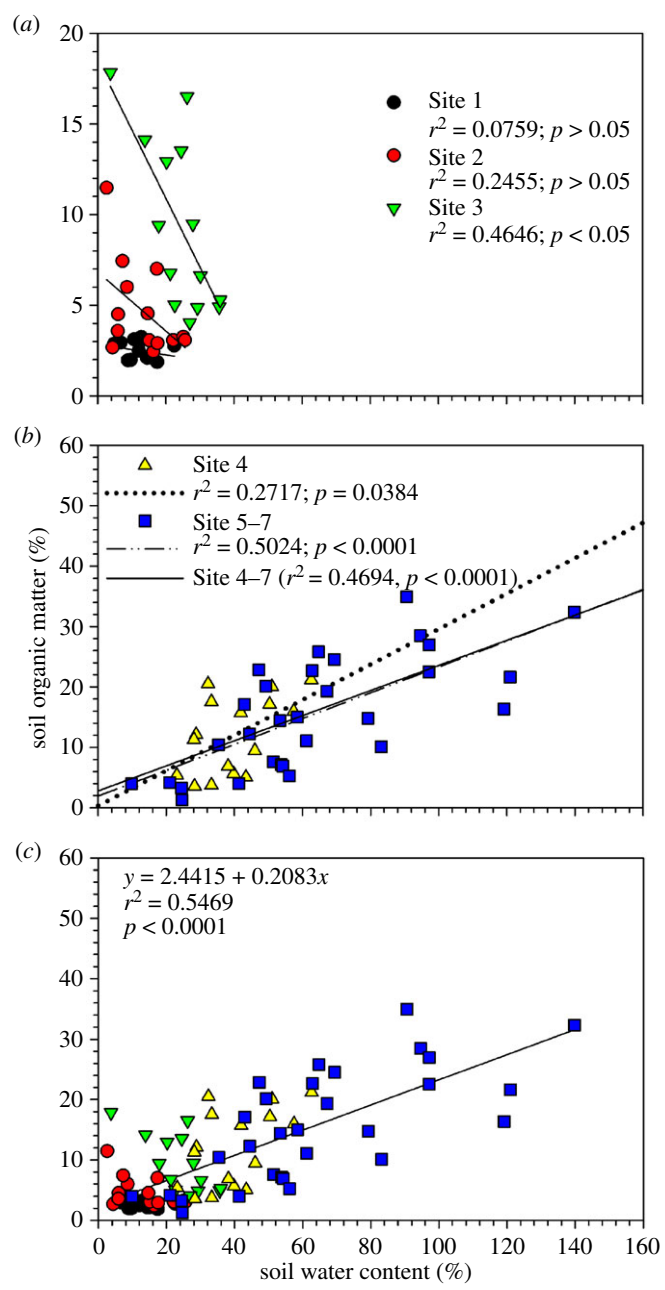


**Figure 6.** Relationship between soil water content (%) and soil organic matter (%) at Sites 1–3 (a), Sites 4–7 (b) and at all sites along the study transect (c) across a seasonal floodplain at Nxaraga. The data are the means of three replicates per sampling site for SWC and SOM obtained during the monthly 2-day sampling campaigns. The SWC–SOM relationship was assessed at site level in (a) and (b) because of the drought condition the seasonal floodplain experienced during the study period which might have affected the littoral sites more than the wetter sites near the Boro channel. (Online version in colour.)

[54], the optimum pH for most methanogenic bacteria is 7.0. However, only 8% of the 112 soil pH measurements along the transect at Nxaraga were between pH 6.7 and 7.3. Approximately 73% of the pH measurements were lower than 6.7, which could mean that methanogens in the floodplain soils have adapted to the slightly acidic conditions such that the highest  $\text{CH}_4$  emissions were

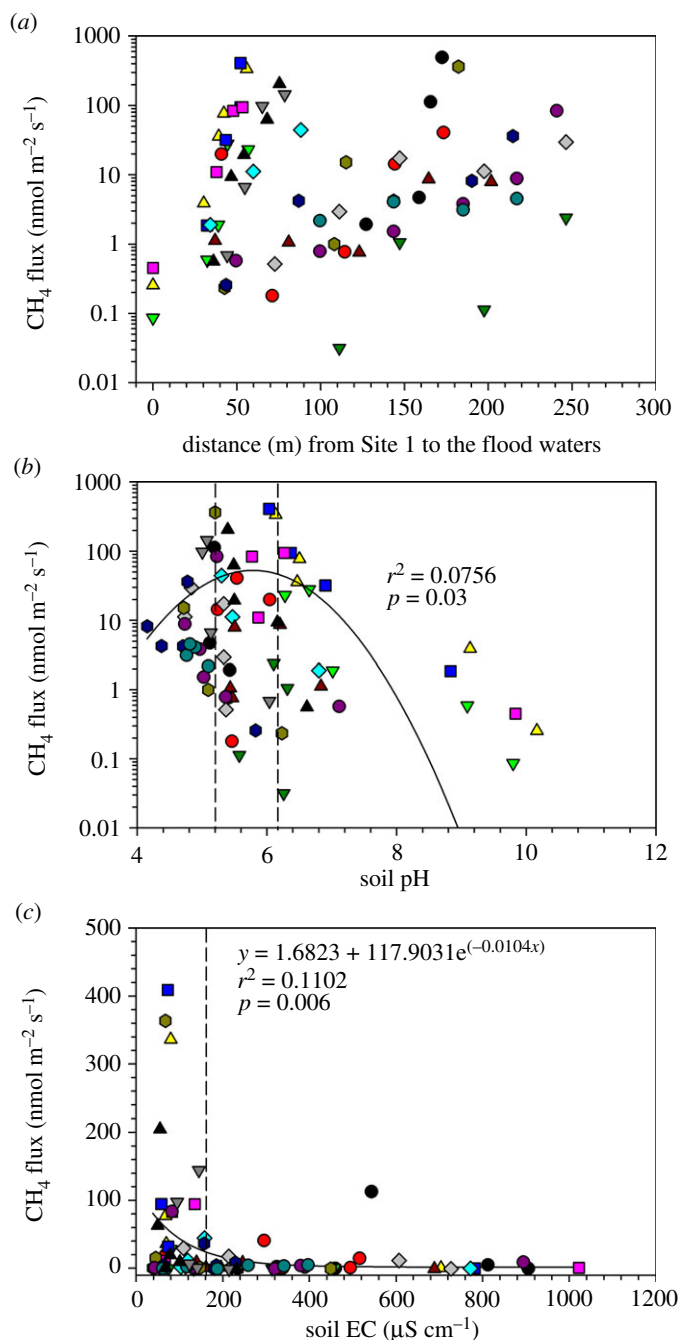


**Figure 7.** Variation of mean monthly CH<sub>4</sub> fluxes with distance along the study transect (a) and its relationship with soil pH (b) and soil EC (c) in a seasonal floodplain at Nxaraga. The data are the means of three replicates per sampling site for soil pH, soil EC and soil CH<sub>4</sub> fluxes obtained during the monthly 2-day sampling campaigns. The dashed lines in (b) and (c) indicate the optimum range of soil pH (pH 5.2–6.2) and soil EC (less than 160 μS cm<sup>-1</sup>) for soil CH<sub>4</sub> flux in the seasonal floodplain at Nxaraga. See figure 2 for legend. (Online version in colour.)

recorded at soil pH between 5.0 and 6.6 (figure 7a) [55]. Much higher soil pH values (8.6–10.5) at Site 1 were probably influenced by the salt deposits at the site (see EC below) and was the only site where CH<sub>4</sub> was oxidized almost consistently throughout the study period, with an average

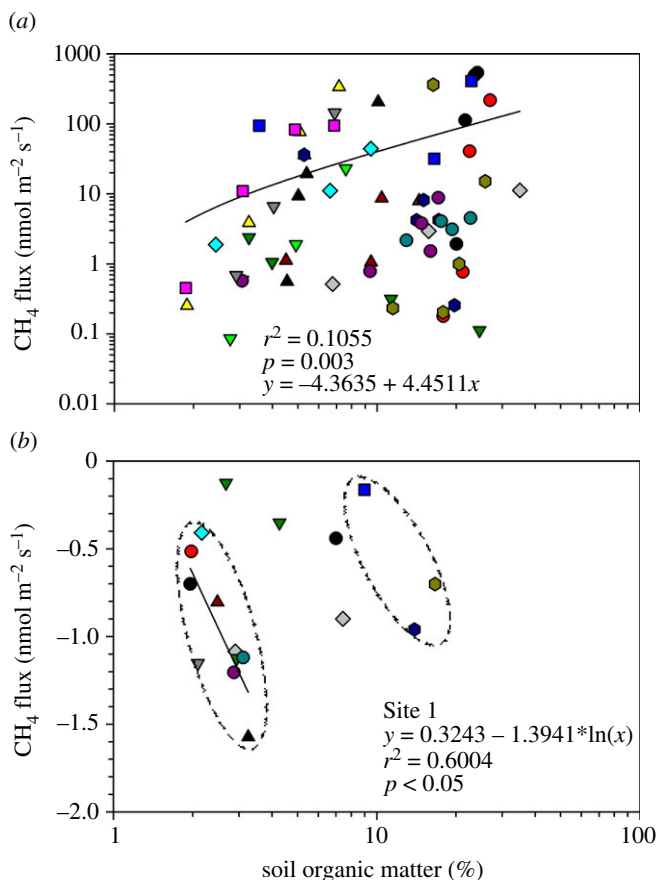


**Figure 8.** Relationship between soil organic matter (%) and  $\text{CH}_4$  emissions (a), and  $\text{CH}_4$  oxidation (b) in a seasonal floodplain at Nxaraga. The data are the means of three replicates per sampling site for SOM and soil  $\text{CH}_4$  fluxes obtained during the monthly 2-day sampling campaigns. The mean monthly  $\text{CH}_4$  oxidation fluxes in (b) were measured at Site 1 (in circles) and at Site 2 (outside the circles). See figure 2 for legend. (Online version in colour.)

flux of  $-0.79 \pm 0.09 \text{ nmol m}^{-2} \text{ s}^{-1}$ . Most methanotrophs operate around neutral pH, except for some species, which have adapted to high alkalinity situations, such as a highly alkaline soda lake (pH 9.5) in Central Asia [56]. Since salt deposits are common in forested island soils in the Okavango Delta, the methanotrophs are likely to have adapted to the high alkalinity in these soil environments.

Water EC, a measure of salinity, generally increases due to evapo-concentration as the flood water traverses the Okavango Delta to distal areas. A significant amount of water in floodplains around forested islands experiences a strong radial flow to the centre of islands induced by evapotranspiration by broad-leaved evergreen trees on the fringes of the islands. The process consequently concentrates solutes in the island fringe soils and in soil water underneath the islands. This permanent burial of solutes beneath islands is the main process that maintains the Okavango Delta as a freshwater ecosystem [33,34]. As the floodwaters recede, some of the remaining solutes are deposited on the rest of the floodplain soils causing an island-floodplain EC gradient (figure 4a). While salinity, defined as  $\text{EC} > 4000 \mu\text{S cm}^{-1}$ , depresses both methanogenic and methanotrophic activities [57], the much lower EC values (this study) measured at Nxaraga floodplain sites did not seem to affect  $\text{CH}_4$  fluxes. Most of the higher fluxes (greater than  $100 \text{ nmol CH}_4 \text{ m}^{-2} \text{ s}^{-1}$ ) were observed at soil  $\text{EC} < 200 \mu\text{S cm}^{-1}$ , while high EC values, measured at the dry soil site, were accompanied by net microbial  $\text{CH}_4$  oxidation.

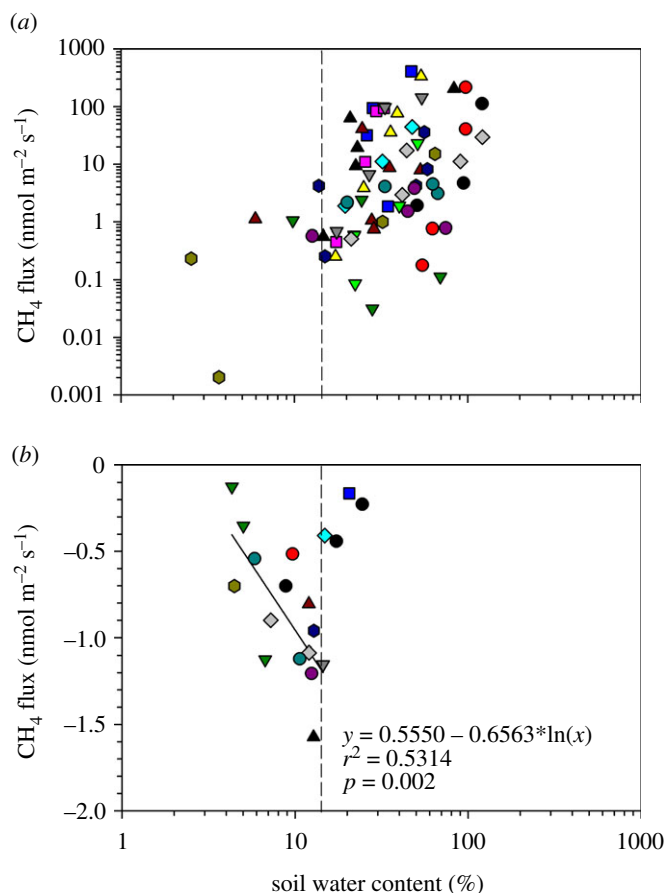


**Figure 9.** Relationship between soil water content and soil CH<sub>4</sub> emissions (a) and CH<sub>4</sub> oxidation (b) in a seasonal floodplain at Nxaraga. The data are the means of three replicates per sampling site for SWC and soil CH<sub>4</sub> fluxes obtained during the monthly 2-day sampling campaigns. The dashed line indicates SWC at which soil CH<sub>4</sub> oxidation (b) is optimum at 15% SWC. See figure 2 for legend. (Online version in colour.)

The importance of SWC and SOM in controlling CH<sub>4</sub> emission and oxidation processes has been presented in literature [58]. CH<sub>4</sub> emission is a net result of its production by methanogens and consumption by methanotrophs in anaerobic and aerobic soils, respectively [55,59]. Figures 8 and 9 show clear effects of SOM and SWC on both CH<sub>4</sub> emission and oxidation in the seasonal floodplain at Nxaraga.

Although the range of soil CH<sub>4</sub> fluxes along the study transect was large, the fluxes increased with SOM in the seasonal floodplain (figure 8a). A significant positive correlation ( $r^2 = 0.1465$ ,  $p < 0.05$ ) was observed between natural-log transformed soil CH<sub>4</sub> flux and SOM data (figure not shown). The high CH<sub>4</sub> fluxes increased rapidly to a threshold of about 300–400 nmol m<sup>-2</sup> s<sup>-1</sup> at SOM contents of approximately 7–8% (figure 8a). Soil CH<sub>4</sub> emissions and SOM correlate mainly because the SOM provides substrates for methanogenic CH<sub>4</sub> production while its decomposition maintains anaerobic soil conditions, by consuming dissolved O<sub>2</sub> and other available alternative electron acceptors such as NO<sub>3</sub><sup>-</sup>, Fe<sup>3+</sup>, Mn<sup>4+</sup> and SO<sub>4</sub><sup>2-</sup> [60]. Soil CH<sub>4</sub> emissions were found to be strongly correlated to SWC between the ranges 15–150% (figure 9a). An optimum SWC for CH<sub>4</sub> emission has been, therefore, estimated at 50%, beyond which SWC appears to suppress soil CH<sub>4</sub> emission by constraining the diffusivity of CH<sub>4</sub> to the atmosphere (figure 9a). However, more sampling is needed to confirm the optimum SWC required for soil CH<sub>4</sub> emissions by sampling

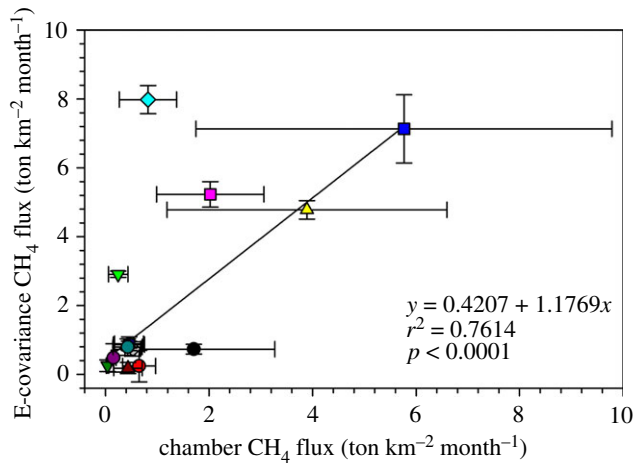


**Figure 10.** Correlation between chamber CH<sub>4</sub> fluxes and EC-CH<sub>4</sub> fluxes measured with closed dynamic chamber and eddy-covariance techniques, respectively, at Nxaraga seasonal floodplain in 2018 and 2019. The chamber flux data are the means of chamber Sites 2–7 obtained for each monthly day of sampling. The eddy-covariance flux is the conditional monthly mean of all available data points in the [130°, 270°] wind sector for which 90% of the measured flux originated within 200 m from the instrument mast. This condition was imposed to ensure that the flux footprint of the eddy-covariance system was limited to the portion of the floodplain where chamber sampling occurred. CH<sub>4</sub> flux for November 18 (see legend in figure 4) was excluded for curve fitting. (Online version in colour.)

multiple seasonal floodplains because it is an important environmental factor for modelling CH<sub>4</sub> emissions in the Okavango Delta and potentially further afield.

Once emitted, the CH<sub>4</sub> may remain in the atmosphere where it acts as a potent GHG with a global warming potential 28 times that of CO<sub>2</sub>, or it may diffuse into the dry soil matrix with subsequent oxidation to CO<sub>2</sub> by methanotrophic bacteria. The widespread aerobic microbial CH<sub>4</sub> oxidation which occurs primarily within the top 10 cm layer of undisturbed soils [61–63] is the only known biological sink of this GHG and accounts for 4–6% of the total global CH<sub>4</sub> sink strength [17]. Soil CH<sub>4</sub> oxidation, therefore, has a direct effect on net CH<sub>4</sub> emissions from the environment. The rate of soil CH<sub>4</sub> oxidation depends on the microbial activity of methanotrophs and the rate of diffusion of atmospheric CH<sub>4</sub> within the soil profile [64,65]. The microbial CH<sub>4</sub> oxidation process, just like CH<sub>4</sub> production by methanogens, is regulated by a number of environmental factors such as SWC, SOM, temperature, pH and soil nitrogen content [59,66]. The rate of diffusion of atmospheric CH<sub>4</sub> and O<sub>2</sub> into the soil matrix for CH<sub>4</sub> oxidation is controlled primarily by SWC and the physical soil structure (e.g. soil texture and compaction) such that waterlogged and fine-textured soils, for instance, have low gas diffusivity [59,65]. In fact, gas transport into the soil matrix has been suggested to be the main rate limiting factor for atmospheric CH<sub>4</sub> oxidation in soils [67]. In the current study, although SWC and SOM at Site 1 varied within a narrow range, soil CH<sub>4</sub> oxidation at the site increased with both SOM (figure 8*b*) and SWC (figure 9*b*). The optimum SWC for CH<sub>4</sub> oxidation (where more negative fluxes were observed) in dry soils at Nxaraga was estimated at approximately 15% (figure 9*b*): lower and higher SWC values seem to suppress CH<sub>4</sub> oxidation, either by physiological water stress of methanotrophs at very low SWC or by restricting supply of both CH<sub>4</sub> and O<sub>2</sub> required for aerobic soil methanotrophic activity at higher SWC [58,65]. The optimum SWC of 15% for soil CH<sub>4</sub> oxidation observed at Nxaraga is consistent with optimum SWCs for methanotrophic activities reported in previous studies: 11% SWC in Whalen *et al.* [68] and 20% SWC in Castro *et al.* [69]. The variation has been suggested to primarily depend on soil type [70]. Figure 9*a* further suggests that SWC values between 15% and 50% enhance CH<sub>4</sub> emission, rather than oxidation, from the seasonal floodplain soils because as SWC increases, it simultaneously creates conducive anaerobic conditions for CH<sub>4</sub> production

when substrates are available and lowers its oxidation rate by restricting O<sub>2</sub> supply into the soil [55,59]. It was not possible to estimate the optimum SOM for soil CH<sub>4</sub> oxidation from the data currently available for the Delta, and therefore calls for more research on the effect of SOM and other environmental factors, including soil inorganic nitrogen concentration, not assessed in this study.

## 5. Upscaling of CH<sub>4</sub> emission and oxidation rates to the whole Okavango Delta

The mean CH<sub>4</sub> emission rate measured by closed chambers at Nxaraga ( $44.89 \pm 10.80 \text{ nmol m}^{-2} \text{ s}^{-1}$ , equivalent to  $2.61 \pm 0.62 \text{ mg CH}_4 \text{ m}^{-2} \text{ h}^{-1}$ ) is comparable with emissions from several tropical wetlands across the world (range  $0.003\text{--}40.4 \text{ mg CH}_4 \text{ m}^{-2} \text{ h}^{-1}$  and mean of  $7.67 \text{ mg CH}_4 \text{ m}^{-2} \text{ h}^{-1}$ ), including the Congo River Basin with a CH<sub>4</sub> flux of  $4.41 \text{ mg m}^{-2} \text{ h}^{-1}$  [71]. The mean CH<sub>4</sub> flux rate at Nxaraga is also comparable to fluxes from 71 northern, temperate and subtropical wetlands where mean fluxes were reported at  $2.01 \pm 0.16 \text{ mg CH}_4 \text{ m}^{-2} \text{ h}^{-1}$  for subtropical,  $3.03 \pm 0.05 \text{ mg CH}_4 \text{ m}^{-2} \text{ h}^{-1}$  for boreal,  $4.54 \pm 0.19 \text{ mg CH}_4 \text{ m}^{-2} \text{ h}^{-1}$  for temperate and  $4.68 \pm 0.26 \text{ mg CH}_4 \text{ m}^{-2} \text{ h}^{-1}$  for subarctic wetlands [72]. A more recent analysis of global natural wetlands estimated CH<sub>4</sub> emissions at  $2.01 \text{ mg CH}_4 \text{ m}^{-2} \text{ h}^{-1}$  (range  $1.37\text{--}2.43$ ) [15]. Similarly, the soil CH<sub>4</sub> oxidation rates ( $0.046 \pm 0.005 \text{ mg m}^{-2} \text{ h}^{-1}$  observed at Nxaraga are also comparable to mean CH<sub>4</sub> oxidation rates of  $0.13\text{--}2.02 \text{ mg m}^{-2} \text{ h}^{-1}$  recorded in northern, temperate and subtropical wetlands [72].

Although uncertainties of these flux estimates are large, the similarity in CH<sub>4</sub> flux rates observed in different wetlands and parts of the world is noteworthy. Research on CH<sub>4</sub> fluxes from wetlands is generally skewed towards arctic and temperate climate wetlands, with fewer studies from tropical and subtropical climate zones. This imbalance needs to be addressed in order to better model the global CH<sub>4</sub> budget.

Chamber fluxes are representative of small-scale biophysical and biogeochemical processes and spatial heterogeneity can make upscaling to plot or landscape scales challenging, although strong agreements between upscaled chamber fluxes and fluxes derived by other techniques such as eddy-covariance have been reported [73–76]. In this study, a good agreement ( $r^2 = 0.8102$ ,  $p = 0.0002$ ) was also observed using monthly averaged areal CH<sub>4</sub> fluxes in 2018 and 2019 from the chamber and eddy-covariance techniques (figure 10).

Gumbrecht *et al.* [25] estimated the total area of the Okavango wetland at  $13\,693 \text{ km}^2$ , about 22%, 24% and 54% of which are permanently, seasonally and occasionally flooded areas of the system. These figures have been recently revisited to take into account the climatic and developmental changes the Okavango basin, which includes the Delta, has experienced over the past two decades. While seasonal floodplains are inundated almost annually, occasional floodplains are flooded only during high floods, which occur approximately once in a decade, and can, therefore, be considered as dry areas capable of CH<sub>4</sub> oxidation as observed at inland Site 1 in this study. Assuming that Site 1 at Nxaraga (where CH<sub>4</sub> oxidation > CH<sub>4</sub> production) is a proxy for the occasionally flooded wetlands and that Sites 2–7 (where CH<sub>4</sub> production > CH<sub>4</sub> oxidation) are representative of seasonal floodplains in the Okavango Delta, we estimate the net CH<sub>4</sub> emission for these two hydrological zones to be of the order of  $0.072 \pm 0.016 \text{ Tg a}^{-1}$  with net emissions at seasonal swamps of  $0.075 \pm 0.018 \text{ Tg a}^{-1}$  and net oxidation in occasional swamps of the order of  $2.817 \times 10^{-3} \pm 0.307 \times 10^{-3} \text{ Tg a}^{-1}$ . These estimates suggest that the biological CH<sub>4</sub> sink in the occasional floodplain soils in the Delta is small as it accounts for only 4% of the total CH<sub>4</sub> emissions in the seasonal floodplains in the wetland. The fraction of the atmospheric CH<sub>4</sub> associated with the biological sink in the Okavango Delta is, however, comparable to the global average sink of 4–6% [17]. There is, however, need for more research in soil CH<sub>4</sub> oxidation in the Delta since the current study sampled only one site that may not adequately represent the vast areas of the occasionally flooded wetlands of the system.

## 6. Conclusion

This study estimated chamber-based CH<sub>4</sub> emission and oxidation rates in a seasonal floodplain in the Okavango Delta at  $44.89 \pm 10.80 \text{ nmol m}^{-2} \text{ s}^{-1}$  and  $0.79 \pm 0.09 \text{ nmol m}^{-2} \text{ s}^{-1}$ , respectively. Although measurements were done during a relatively dry period for the Delta, the observed CH<sub>4</sub> fluxes are comparable to fluxes in other wetlands across the world. The observed CH<sub>4</sub> oxidation which was upscaled to the whole dry occasionally flooded swamp area of the Okavango Delta accounted for approximately 4% of the total CH<sub>4</sub> emissions from the Delta's seasonal floodplains. The Delta's CH<sub>4</sub> sink due to methanotrophic activity is also comparable to the global average biological sink of 4–6%. As in other wetlands, SWC followed by SOM were found to be the main environmental factors controlling CH<sub>4</sub> fluxes in seasonal swamps in the Delta. Maximum CH<sub>4</sub> emission and oxidation rates in the seasonal floodplain at Nxaraga were observed at 50% and 15% SWC, respectively. EC and pH were not correlated with CH<sub>4</sub> fluxes in the seasonal floodplains. Upscaling of CH<sub>4</sub> oxidation fluxes were achieved from measurements at only one dry soil site. Future studies should, therefore, attempt to measure CH<sub>4</sub> oxidation fluxes at several dry soil sites in different drylands (e.g. grasslands, woodlands, forests) of the Okavango Delta.

**Data accessibility.** The data that are used in this paper are provided as electronic supplementary material.

**Authors' contributions.** M.J.G., C.H., M.M.-H., U.M.S. were involved in project conception, sample and data collection, sample and data analysis and manuscript writing. E.M. was involved in data collection and manuscript writing K.B.M. was involved in data collection and manuscript writing P.E.L. was involved in data analysis and manuscript writing A.M. was involved in generating maps and methods.

**Competing interests.** We declare we have no competing interests.

**Funding.** This work was funded by the UK Natural Environment Research Council (NERC) through the Global Methane Budget project (grant nos. NE/N015746/1 and NE/N015746/2)..

**Acknowledgements.** We thank the UK Centre for Ecology and Hydrology (UKCEH) for availing research equipment. We also thank the Okavango Research Institute and its Environmental Laboratory for additional research equipment, field logistics and sample analysis.

## References

1. IPCC. 1996 Climate change 1995: the science of climate change: contribution of working group I to the second assessment report of the intergovernmental panel on climate change (eds JT Houghton, LG Meira Filho, BA Callander, N Harris, A Kattenberg, K Maskell), pp. 572. Cambridge, UK: Cambridge University Press.
2. Wang Z, Zeng D, Patrick WH. 1996 Methane emissions from natural wetlands. *Environ. Monit. Assess.* **42**, 143–161. (doi:10.1007/BF00394047)
3. Johansson AE, Gustavsson A-M, Oquist MG, Svensson BH. 2004 Methane emissions from a constructed wetland treating wastewater - seasonal and spatial distribution and dependence on edaphic factors. *Water Res.* **38**, 3960–3970. (doi:10.1016/j.watres.2004.07.008)
4. Nahlik AM, Mitsch WJ. 2011 Methane emissions from tropical freshwater wetlands located in different climatic zones of Costa Rica. *Glob. Change Biol.* **17**, 1321–1334. (doi:10.1111/j.1365-2486.2010.02190.x)
5. Dlugokencky EJ, Houweling S, Bruhwiler L, Masarie KA, Lang PM, Miller JB, Tans PP. 2003 Atmospheric methane levels off: temporary pause or a new steady-state? *Geophys. Res. Lett.* **30**, 1992. (doi:10.1029/2003GL018126)
6. Turner AJ, Frankenberg C, Wennberg PO, Jacob DJ. 2017 Ambiguity in the causes for decadal trends in atmospheric methane and hydroxyl. *Proc. Natl Acad. Sci. USA* **114**, 5367–5372. (doi:10.1073/pnas.1616020114)
7. Rigby M *et al.* 2008 Renewed growth of atmospheric methane. *Geophys. Res. Lett.* **35**, L22805. (doi:10.1029/2008GL036037)
8. Dlugokencky EJ *et al.* 2009 Observational constraints on recent increases in the atmospheric CH<sub>4</sub> burden. *Geophys. Res. Lett.* **36**, L18803. (doi:10.1029/2009GL039780)
9. Kirschke S *et al.* 2013 Three decades of global methane sources and sinks. *Nat. Geosci.* **6**, 813–823. (doi:10.1038/ngeo1955)

10. Nisbet EG, Dlugokencky EJ, Bousquet P. 2014 Methane on the rise again. *Science* **343**, 493–495. (doi:10.1126/science.1247828)
11. Bousquet P *et al.* 2011 Source attribution of the changes in atmospheric methane for 2006–2008. *Atmos. Chem. Phys.* **11**, 3689–3700. (doi:10.5194/acpc-10-27603-2010)
12. Bloom AA, Palmer PI, Fraser A, Reay DS, Frankenberg C. 2010 Large-scale controls of methanogenesis inferred from methane and gravity spaceborne data. *Science* **327**, 322–325. (doi:10.1126/science.1175176)
13. Meng L, Paudel R, Hess PGM, Mahowald NM. 2015 Seasonal and interannual variability in wetland methane emissions simulated by CLM4Me' and CAM-chem and comparisons to observations of concentrations. *Biogeosciences* **12**, 4029–4049. (doi:10.5194/bg-12-4029-2015)
14. Saunio M *et al.* 2016 The global methane budget 2000–2012. *Earth Syst. Sci. Data* **8**, 697–751. (doi:10.5194/essd-8-697-2016)
15. Saunio M *et al.* 2020 The global methane budget 2000–2017. *Earth Syst. Sci. Data* **12**, 1561–1623. (doi:10.5194/essd-12-1561-2020)
16. Valenzuela EI *et al.* 2017 Anaerobic methane oxidation driven by microbial reduction of natural organic matter in a tropical wetland. *Appl. Environ. Microbiol.* **83**, e00645-17. (doi:10.1128/AEM.00645-17)
17. Ciais P *et al.* 2013 Carbon and other biogeochemical cycles. In *Climate change 2013: the physical science basis. Contribution of working group I to the fifth assessment report of the intergovernmental panel on climate change* (eds TF Stocker *et al.*), pp. 465–570. Cambridge, UK, Cambridge University Press.
18. McCarthy TS, Ellery WN, Ellery K. 1993 Vegetation-induced, subsurface precipitation of carbonate as an aggradational process in the permanent swamps of the Okavango Delta fan, Botswana. *Chem. Geol.* **107**, 111–131. (doi:10.1016/0009-2541(93)90105-R)
19. SMEC 1987 Southern Okavango integrated water development, phase 1: final report technical study. In *Water resource and development*, vol III. Gaborone, Botswana: Department of Water Affairs.
20. McCarthy TS, Ellery WN. 1998 The Okavango Delta. *Trans. R. Soc. S. Afr.* **53**, 157–182. (doi:10.1080/00359199809520384)
21. Milzow C, Tshkiso O, Kgotlhang L, Kinzelbach W. 2010 Sediment transport monitoring and short term modeling in the Okavango Delta, Botswana. *Wetlands* **30**, 417–428. (doi:10.1007/s13157-010-0042-x)
22. King J, Chonguica E. 2016 Integrated management of the Cubango-Okavango River Basin. *Ecohydrol. Hydrobiol.* **16**, 263–271. (doi:10.1016/j.ecohyd.2016.09.005)
23. Dincer T, Hutton LG, Kupee BBJ. 1981 Study, using stable isotopes, of flow distribution, surface-groundwater relations and evapotranspiration in the Okavango swamp, Botswana. Proc. Ser. SII/AUB/493, pp. 3–26. Vienna, Austria: International Atomic Energy Agency.
24. McCarthy TS, Ellery WN, Stanistreet IG. 1992 Avulsion mechanisms on the Okavango fan, Botswana: the control of a fluvial system by vegetation. *Sedimentology* **39**, 119–195. (doi:10.1111/j.1365-3091.1992.tb02153.x)
25. Gumbrecht T, McCarthy J, McCarthy TS. 2004 Channels, wetlands and islands in the Okavango Delta, Botswana, and their relation to hydrological and sedimentological processes. *Earth Surf. Proc. Land.* **29**, 15–29. (doi:10.1002/esp.1008)
26. Mladenov N, McKnight DM, Wolski P, Murray-Hudson M. 2007 Simulation of DOM fluxes in a seasonal floodplain of the Okavango Delta, Botswana. *Ecol. Model.* **205**, 181–195. (doi:10.1016/j.ecolmodel.2007.02.015)
27. Bonyongo MC, Bredenkamp GJ, Veenendaal E. 2000 Floodplain vegetation in the Nxaraga Lagoon area, Okavango Delta, Botswana. *S. Afr. J. Bot.* **66**, 15–21. (doi:10.1016/S0254-6299(15)31046-2)
28. Ellery K, Ellery WN, Rogers KH, Walker BH. 1991 Water depth and biotic insulation: major determinants of back-swamp plant community composition. *Wetl. Ecol. Manag.* **1**, 149–162. (doi:10.1007/BF00177289)
29. Heinl M, Neuenschwander A, Sliva J, Vanderpost C. 2006 Interactions between fire and flooding in a southern African floodplain system (Okavango Delta, Botswana). *Landsc. Ecol.* **21**, 699–709. (doi:10.1007/s10980-005-5243-y)



30. Ramberg L, Wolski P, Krah M. 2006 Water balance and infiltration in a seasonal floodplain in the Okavango Delta, Botswana. *Wetlands* **26**, 677–690. (doi:10.1672/0277-5212(2006)26[677:WBAIIA]2.0.CO;2)
31. Heinl M, Sliva J, Tacheba B, Murray-Hudson M. 2008 The relevance of fire frequency for the floodplain vegetation of the Okavango Delta, Botswana. *Afr. J. Ecol.* **46**, 350–358. (doi:10.1111/j.1365-2028.2007.00847.x)
32. SMEC. 1989 *Ecological zoning Okavango Delta. Final report volume 1 - main report*. Kalahari conservation society. Botswana, Southern Africa: Gaborone.
33. Bauer P, Supper R, Zimmermann S, Kinzelbach W. 2006 Geoelectrical imaging of groundwater salinization in the Okavango Delta, Botswana. *J. Appl. Geophys.* **60**, 126–141.
34. Ramberg L, Wolski P. 2008 Growing islands and sinking solutes: processes maintaining the endorheic Okavango Delta as a freshwater system. *Plant Ecol.* **196**, 215–231. (doi:10.1007/s11258-007-9346-1)
35. Heinl M, Frost P, Vanderpost C, Sliva J. 2007 Fire activity on drylands and floodplains in the southern Okavango Delta, Botswana. *J. Arid Environ.* **68**, 77–87. (doi:10.1016/j.jaridenv.2005.10.023)
36. Riley WJ, Subin ZM, Lawrence DM, Swenson SC, Torn MS, Meng L, Mahowald NM, Hess P. 2011 Barriers to predicting changes in global terrestrial methane fluxes: analyses using CLM4Me, a methane biogeochemistry model integrated in CESM. *Biogeosciences* **8**, 1925–1953. (doi:10.5194/bg-8-1925-2011)
37. Staring GJ. 1978 Soils of the Okavango Delta, Field Document No. 14: Swamp and dryland soils of the Okavango. Project BOT 72/019, UNDP/FAO and Government of Botswana (report and maps).
38. De Wit PV, Nachtergaele FO. 1990 Explanatory note on the soil map of the Republic of Botswana. Ministry of Agriculture, Soil Mapping and Advisory Service Project, BOT/85/011: FAO, UNDP/Government of Botswana, Gaborone, Botswana.
39. Hensen A, Skiba U, Famulari D. 2013 Low cost and state of the art methods to measure nitrous oxide emissions. *Environ. Res. Lett.* **8**, 025022. (doi:10.1088/1748-9326/8/2/025022)
40. Gondwe MJ, Masamba WR. 2014 Spatial and temporal dynamics of diffusive methane emissions in the Okavango Delta, northern Botswana, Africa. *Wet. Ecol. Manag.* **22**, 63–78. (doi:10.1007/s11273-013-9323-5)
41. Helfter C, Gondwe MJ, Murray-Hudson M, Makati A, Lunt MF, Palmer PI, Skiba U. Submitted. Phenology of emergent macrophytes is the dominant control of methane emissions in a tropical non-forested wetland. *Nat. Commun.*
42. Pedersen AR, Petersen SO, Schelde K. 2010 A comprehensive approach to soil-atmosphere trace-gas flux estimation with static chambers. *Eur. J. Soil Sci.* **61**, 888–902. (doi:10.1111/j.1365-2389.2010.01291.x)
43. Levy PE *et al.* 2012 Methane emissions from soils: synthesis and analysis of a large UK data set. *Glob. Change Biol.* **18**, 1657–1669. (doi:10.1111/j.1365-2486.2011.02616.x)
44. Hendershot WH, Lalonde H, Duquette M. 2007 Soil reaction and exchangeable acidity. In *Soil sampling and methods of analysis* (eds MR Carter, EG Gregorich), pp. 173–1178, 2nd. Boca Raton, Florida: CRC Press.
45. Miller JJ, Curtin D. 2007 Electrical conductivity and soluble ions. In *Soil sampling and methods of analysis* (eds MR Carter, EG Gregorich), pp. 161–171, 2nd. Boca Raton, Florida: CRC Press.
46. Schulte EE, Hopkins BG. 1996 Estimation of organic matter by weight loss-on-ignition. In *Soil organic matter: analysis and interpretation* (eds FR Magdoff *et al.*), pp. 21–31. Madison, WI: SSSA.
47. Wolski P, Murray-Hudson M, Thito K, Cassidy L. 2017 Keeping it simple: monitoring flood extent in large data-poor wetlands using MODIS SWIR data. *Int. J. Appl. Earth Obs. Geoinf.* **57**, 224–234. (doi:10.1016/j.jag.2017.01.005)
48. Chamberlain SD, Hemes KS, Eichelmann E, Szutu DJ, Verfaillie JG, Baldocchi DD. 2020 Effect of drought-induced salinization on wetland methane emissions, gross ecosystem productivity, and their interactions. *Ecosystems* **23**, 675–688. (doi:10.1007/s10021-019-00430-5)
49. Moore BD, Kaur G, Motavalli PP, Zurweller BA, Svoma BM. 2017 Soil greenhouse gas emissions from agroforestry and other land uses under different moisture regimes in lower Missouri River floodplain soils: a laboratory approach. *Agrofor. Syst.* **92**, 335–348. (doi:10.1007/s10457-017-0083-8)
50. Valentine DW, Holland EA, Schimel DS. 1994 Ecosystem and physiological controls over methane production in northern wetlands. *J. Geophys. Res.* **99**, 1563–1571. (doi:10.1029/93JD00391)

51. Moore TR, Knowles R. 1990 Methane emissions from fen, bog and swamp peatlands in Quebec. *Biogeochemistry* **11**, 45–61. (doi:10.1007/BF00000851)
52. Wen X, Yang S, Horn F, Winkel M, Wagner D, Liebner S. 2017 Analysis of methanogenic archaea identifies community-shaping environmental factors of natural environments. *Front. Microbiol.* **8**, 1339. (doi:10.3389/fmicb.2017.01339)
53. Bonyongo MC, Mubyana T, Totolo O, Veenandaal EM. 2002 Flooding and soil nutrient status in the Okavango Delta's seasonal floodplains. *Botsw. Notes Rec.* **34**, 123–130.
54. Segers R. 1998 Methane production and methane consumption: a review of processes underlying wetland methane fluxes. *Biogeochemistry* **41**, 23–51. (doi:10.1023/A:1005929032764)
55. Le Mer J, Roger P. 2001 Production, oxidation, emission and consumption of methane by soils: a review. *Eur. J. Soil Biol.* **37**, 25–50. (doi:10.1016/S1164-5563(01)01067-6)
56. Khmelenina VN, Kalyuzhnaya MG, Starostina NG, Suzina NE, Trotsenko YA. 1997 Isolation and characterization of halotolerant alkaliphilic methanotrophic bacteria from Tuva soda lakes. *Curr. Microbiol.* **35**, 257–261. (doi:10.1007/s002849900249)
57. van der Gon HACD, Neue H-U. 1995 Methane emission from a wetland rice field as affected by salinity. *Plant Soil* **170**, 307–313. (doi:10.1007/BF00010483)
58. van den Pol-van Dasselaar A, van Beusichem ML, Oenema O. 1998 Effects of soil moisture content and temperature on methane uptake by grasslands on sandy soils. *Plant Soil* **204**, 213–222. (doi:10.1023/A:1004371309361)
59. Chowdhury TR, Dick RP. 2013 Ecology of aerobic methanotrophs in controlling methane fluxes from wetlands. *Appl. Soil Ecol.* **65**, 8–22. (doi:10.1016/j.apsoil.2012.12.014)
60. Heintze G, Eickenscheidt T, Schmidhalter U, Drösler M. 2017 Influence of soil organic carbon on greenhouse gas emission potential after application of biogas residues or cattle slurry: results from a pot experiment. *Pedosphere* **27**, 807–821. (doi:10.1016/S1002-0160(17)60388-6)
61. Adamsen APS, King GM. 1993 Methane consumption in temperate and subarctic forest soils: rates, vertical zonation, and responses to water and nitrogen. *Appl. Environ. Microbiol.* **59**, 485–490. (doi:10.1128/AEM.59.2.485-490.1993)
62. Koschorreck M, Conrad R. 1993 Oxidation of atmospheric methane in soil: measurements in the field, in soil cores and in soil sample. *Glob. Biogeochem. Cycles* **7**, 109–121. (doi:10.1029/92GB02814)
63. Kruse CW, Moldnup P, Iversen N. 1996 Modelling diffusion and reaction in soils, II, atmospheric methane diffusion and consumption in soils. *Soil Sci.* **161**, 355–365. (doi:10.1097/00010694-199606000-00002)
64. Dörr H, Katruff L, Levin I. 1993 Soil texture parameterization of the methane uptake in aerated soils. *Chemosphere* **26**, 697–713. (doi:10.1016/0045-6535(93)90454-D)
65. Lang R, Goldberg SD, Blagodatsky S, Piepho H-P, Hoyt AM, Harrison RD, Xu J, Cadisch G. 2020 Mechanism of methane uptake in profiles of tropical soils converted from forest to rubber plantations. *Soil Biol. Biochem.* **145**, 107796. (doi:10.1016/j.soilbio.2020.107796)
66. Oertel C, Matschullat J, Zurba K, Zimmermann F, Erasmí S. 2016 Greenhouse gas emissions from soils - a review. *Chem. Erde* **76**, 327–352. (doi:10.1016/j.chemer.2016.04.002)
67. Topp E, Pattey E. 1997 Soils as sources and sinks for atmospheric methane. *Can. J. Soil Sci.* **77**, 167–178. (doi:10.4141/S96-107)
68. Whalen SC, Reeburgh WS, Sandbeck KA. 1990 Rapid methane oxidation in a landfill cover soil. *Appl. Environ. Microbiol.* **56**, 3405–3411. (doi:10.1128/aem.56.11.3405-3411.1990)
69. Castro MS, Steudler PA, Melillo JM. 1995 Factors controlling atmospheric methane consumption by temperate forest soils. *Glob. Biogeochem. Cycles* **9**, 1–10. (doi:10.1029/94GB02651)
70. Schnell S, King GM. 1996 Responses of methanotrophic activity in soils and cultures to water stress. *Appl. Environ. Microbiol.* **62**, 3203–3209. (doi:10.1128/aem.62.9.3203-3209.1996)
71. Sjögersten S, Black R, Evers S, Hoyos-Santillan J, Wright EL, Turner BL. 2014 Tropical wetlands: a missing link in the global carbon cycle? *Glob. Biogeochem. Cycles* **28**, 1371–1386. (doi:10.1002/2014GB004844)
72. Turetsky MR *et al.* 2014 A synthesis of methane emissions from 71 northern, temperate, and subtropical wetlands. *Glob. Change Biol.* **20**, 2183–2197. (doi:10.1111/gcb.12580)

73. Riutta T, Laine J, Aurela M, Rinne J, Vesala T, Laurila T, Haapanala S, Pihlatie M, Tuittila E-S. 2007 Spatial variation in plant community functions regulates carbon gas dynamics in boreal fen ecosystem. *Tellus* **59B**, 838–852. (doi:10.1111/j.1600-0889.2007.00302.x)
74. Sachs T, Giebels M, Boike J, Kutzbach L. 2010 Environmental controls of CH<sub>4</sub> emission from polygonal tundra on the micro-site scale, Lena River Delta, Siberia. *Glob. Change Biol.* **16**, 3096–3110. (doi:10.1111/j.1365-2486.2010.02232.x)
75. Schrier-Uijl AP, Kroon PS, Hensen A, Leffelaar PA, Berendse F, Veenendaal EM. 2010 Comparison of chamber and eddy covariance-based CO<sub>2</sub> and CH<sub>4</sub> emission estimates in a heterogeneous grass ecosystem on peat. *Agric. For. Meteorol.* **150**, 825–831. (doi:10.1016/j.agrformet.2009.11.007)
76. Levy P, Drewer J, Jammot M, Leeson S, Friborg T, Skiba U, van Oije M. 2020 Inference of spatial heterogeneity in surface fluxes from eddy covariance data: a case study from a subarctic mire ecosystem. *Agric. For. Meteorol.* **280**, 107783. (doi:10.1016/j.agrformet.2019.107783)